

New polypyrrole-multiwall carbon nanotubes hybrid materials

R. TURCU^{*}, AL. DARABONT^a, A. NAN, N. ALDEA, D. MACOVEI^b, D. BICA^c, L. VEKAS^c, O. PANA, M. L. SORAN, A. A. KOOS^d, L. P. BIRO^d

National Institute R&D of Isotopic and Molecular Technologies, P. O. Box 700, RO-400293, Cluj-Napoca, Romania

^aBabes-Bolyai University, Faculty of Physics, Cluj-Napoca, Romania

^bRomanian Academy, Timisoara Branch, Magnetic Fluids Laboratory, Timisoara, Romania

^cNational Institute R&D of Materials Physics, P. O. Box MG-7 Bucuresti-Magurele, Romania

^dHungarian Academy of Sciences, Research Institute for Technical Physics and Materials Science, P.O. Box 49, H-1525, Budapest, Hungary

We report the synthesis and characterization of new hybrid materials based on conducting polypyrrole (PPY) and multi wall carbon nanotubes (MWCNTs). MWCNTs were prepared by spray-pyrolysis of liquid hydrocarbon-ferrocene solution in an Ar atmosphere. The composites (PPY-CNT) were obtained by *in-situ* chemical oxidative polymerization of pyrrole in aqueous solution containing MWCNTs. The addition of a water based Fe₃O₄ nanofluid to the polymerization solution results in the formation of a new hybrid nanostructure of MWCNTs coated with PPY containing magnetic nanoparticles. The properties of PPY composites were investigated by TEM, SEM, FTIR spectroscopy and X-ray diffraction (XRD) measurements. MWCNTs covered with PPY have a rough surface, containing some globular forms typical for the polymer. Significant differences between IR spectra for PPY and PPY-CNT nanocomposites appear for the bands ascribed to pyrrole ring vibrations, suggesting that an interaction between the polymer and CNT occurs and this could change the polymer conformation. XRD analysis shows that the crystalline structure of MWCNTs doesn't change significantly by the association with conducting PPY.

(Received January 18, 2006; accepted March 23, 2006)

Keywords: Conducting polymer, Carbon nanotubes, Hybrid materials

1. Introduction

The association of conducting polymers with carbon nanotubes represents a new strategy to obtain composites possessing the properties of each component with a synergistic effect and showing great potential applications as supercapacitors, actuators, biosensors, electromagnetic shielding, electronic devices [1]. Among conducting polymers, polypyrrole have been successfully used for the synthesis of composites with carbon nanotubes, due to its properties such as high conductivity, good stability and easy preparation [2-4]. In this work we report the synthesis of carbon nanotubes (CNT) and polypyrrole (PPY)-CNT nanocomposites by using *in situ* chemical oxidative polymerization of pyrrole in the presence of carbon nanostructures.

2. Experimental

Multi-walled and single-walled CNTs were obtained by chemical vapor deposition from hydrocarbons in the presence of a metal catalyst [5,6]. Two methods may be used to introduce the carbon source material into the pyrolysis furnace: the method of vapors in a gas stream (usually Ar) [5] or the liquid injection method using an atomizer (sprayer) [6]. A single step synthetic route, which

involves the spray-pyrolysis of ferrocene as catalyst dissolved in liquid hydrocarbon (e.g. benzene, xylene) as carbon source, in an Ar atmosphere was performed. The synthesis was carried out at temperatures around 975 °C and at different Ar flow-rates [6]. The liquid hydrocarbon-ferrocene solution is introduced into the sprayer and pulverized into the reaction chamber by the Ar gas flowing around the nozzle. This method has the advantage that the catalyst is simultaneously introduced with the carbon source into the reactor. In the fixed-bed method, the catalyst is put into the reactor at the beginning of the CNTs synthesis [5]. The hydrocarbon, carried over the catalyst by an inert gas, is decomposed on the catalyst and allows the catalytic growth of carbon nanotubes. Carbon nanofibers, single-wall nanotubes (SWCNT), multi-wall nanotubes (MWCNT) were obtained by using the fixed-bed method. After the purification process, a part of CNTs were treated in a hot mixture of acids, namely HNO₃:H₂SO₄ (1:1), for 1h.

The synthesis of the reported PPY-CNT nanocomposites was carried out using the *in situ* chemical polymerization of pyrrole monomer in aqueous solution containing dispersed MWCNTs. In our experiments, both type of acids treated and untreated MWCNTs were used.

A solution of 10 ml deionized water and 0.1g MWCNTs previously treated in acids was sonicated for 1h. When untreated MWCNTs were used we also added dodecylbenzensulfonic acid (DBS) or the Fe_3O_4 nanofluid into the water suspension of MWCNTs. Then, 0.1 ml pyrrole was added to the respective suspension and sonicated for 15 min. The pyrrole monomer/MWCNTs mass ratio was 1, and the oxidant/monomer molar ratio was 0.2 for the reported nanocomposites. An aqueous solution of the oxidant, ammonium persulfate (APS), was slowly added drop wise to the above mixture. The polymerization of the reported samples was performed by using an oxidant/monomer molar ratio of 0.2. The reaction proceeded under magnetic stirring for 10 h at $0 - 5^\circ\text{C}$. A flask of methanol was finally added to terminate the polymerization reaction of pyrrole. The resulting black precipitate was separated by centrifugation, washed with deionized water and methanol and dried at 60°C for 24 h.

The following notations will be used for the PPY nanocomposites: the denomination "*a PPY-CNT*" is used for the sample prepared by using MWCNTs previously treated in acids, the denomination "*b PPY-CNT*" for samples prepared by using MWCNTs untreated in acids with DBS addition in the polymerization solution (DBS/pyrrole=0.5 molar ratio) and the denomination "*c PPY-CNT*" for the samples prepared by using MWCNTs untreated in acids with additional of Fe_3O_4 nanofluid in the polymerization solution.

The morphology of CNTs and PPY-CNT nanocomposites was determined by TEM and SEM using JSM 5600 LV and 1010 JEOL microscopes respectively.

FTIR spectroscopy of the nanocomposites was carried out on a JASCO FTIR 610 spectrophotometer in the range $400-4000\text{ cm}^{-1}$.

Structural characterization of CNTs and PPY-CNT nanocomposites was performed by X-ray diffraction (XRD) using a horizontal powder diffractometer in Bragg-Brentano (BB) geometry with Ni filtered $\text{CuK}\alpha$ radiation, $\lambda = 1.54178\text{ \AA}$. The typical experimental condition was: 10 sec. for each step, initial angle $2\theta = 10$ degree, step 0.05 degree respectively and each profile was measured on 1600 points.

3. Results and discussion

The TEM image presented in Fig. 1 shows that the carbon nanotubes, prepared by spray-pyrolysis of xylene-ferrocene solution, were truly obtained. Field Emission Scanning Electron Microscopy (FESEM) image shown in Fig. 2 indicates that large areas of aligned MWCNTs are grown onto the quartz tube walls.

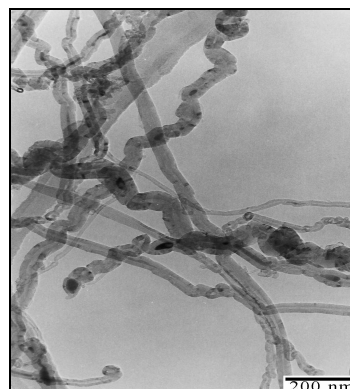


Fig. 1. TEM image of MWCNTs prepared by spray-pyrolysis of liquid hydrocarbon-ferrocene solution.

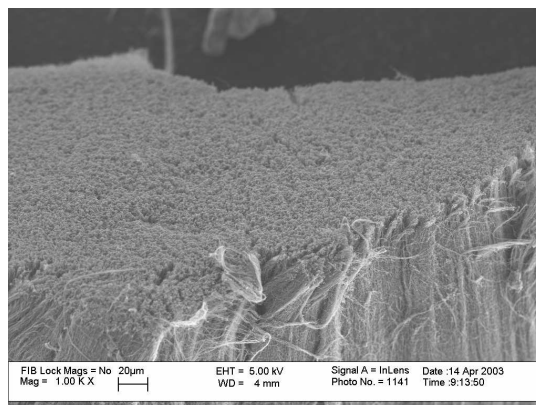


Fig. 2. FESEM image of bundles aligned MWCNTs prepared by spray-pyrolysis of liquid hydrocarbon-ferrocene solution.

The diameters of MWCNTs prepared by spray-pyrolysis of xylene-ferrocene solution are in the range 30-50 nm. One can observe from the Fig. 1 that some catalyst particles remain encapsulated in the MWCNTs even after the purification process. TEM image of the nanocomposite *a PPY-CNT* shows that MWCNTs are coated by a thin layer of PPY, Fig. 3. The MWCNTs covered with PPY have a rough surface, as can be seen from Fig. 4, containing some globular forms typical for the polymer. SEM images for the other nanocomposites (*b PPY-CNT* and *c PPY-CNT*) are similar to that presented in the Fig. 4.

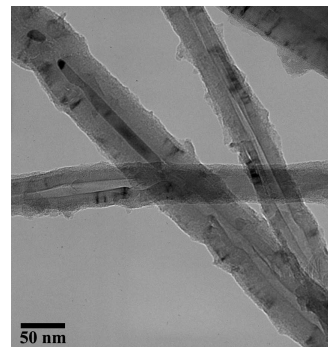


Fig. 3. TEM image of nanocomposite *a PPY-CNT*.

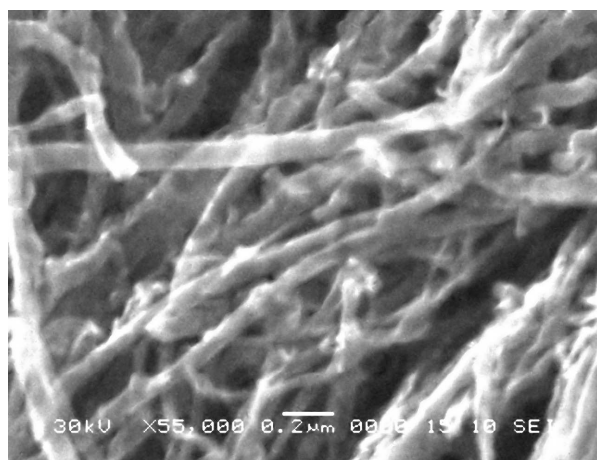


Fig. 4. SEM image of MWCNTs covered with globular PPY.

In Figs. 5 and 6 we can compare the FTIR spectra for DBS doped PPY and for the PPY-CNT nanocomposites prepared using acids treated MWCNTs (sample *a* PPY-CNT) and untreated MWCNTs respectively (sample *b* PPY-CNT). The nanocomposites spectra contain the characteristic absorption bands of PPY in doped state. The IR absorption band positions and their assignments [7,8] for PPY and the nanocomposites are given in the Table 1.

From Table 1 one can observe that significant differences between IR spectra for PPY and PPY-CNT nanocomposites appear for the bands ascribed to pyrrole ring vibrations, located around 790, 900, 1190. These absorption bands are sensitive to the oxidation level and to the conjugation length of the PPY chain [7,8]. The shift of these bands to lower frequencies in the nanocomposites spectra as compared with PPY suggest that an interaction between the polymer and CNT occurs and this could change the polymer conformation.

Table 1. Peak positions (cm^{-1}) of IR absorption bands for pure sample of PPY and nanocomposites PPY-CNT respectively (data from the spectra presented in Figs. 5 and 6).

PPY	<i>a</i> PPY-CNT	<i>b</i> PPY-CNT	Band assignments
791	777	784	ring deformation
864	862		C-H bending
914	901	904	ring deformation
1037	1037	1037	C-H in-plane bend
1198	1181	1178	ring breathing
1295	1294	1300	C-H in-plane bend
1465	1459	1464	ring breathing with contribution from C=C/C-C and C-N
1551	1543	1545	C=C/C-C stretching

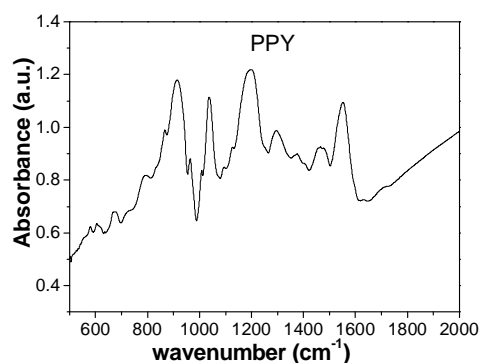


Fig. 5. IR spectrum of PPY doped with DBS.

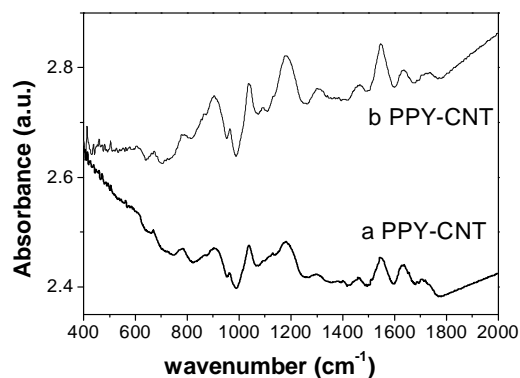


Fig. 6. IR spectra of the nanocomposites: *a* PPY-CNT and *b*-PPY-CNT.

The XRD spectra for MWCNTs and for the nanocomposite sample *c* PPY-CNTs are presented in the Fig. 7. The intense peak around $2\theta = 26.5$ degrees, which appears in both spectra from Fig. 7, is characteristic for the MWCNTs.

The XRD spectrum of *c* PPY-CNTs sample shows peaks for 2θ in the range of 30 – 65 degrees. It represents a characteristic pattern for the XRD in Fe_3O_4 and demonstrates that the magnetic nanoparticles are attached to MWCNTs during the pyrrole polymerization process. At low angles, the XRD spectrum of the nanocomposite contains the contribution from the broad band due to amorphous PPY (Fig. 8).

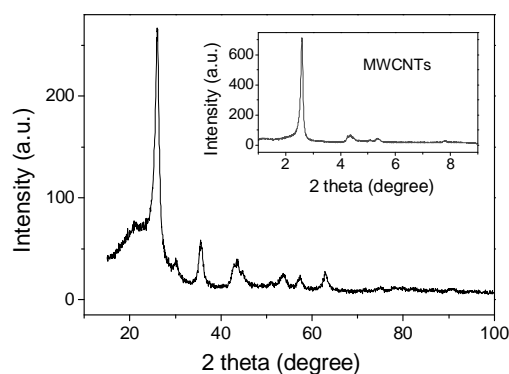


Fig. 7. XRD spectrum for *c* PPY-CNT nanocomposite. Inset: XRD spectrum for MWCNTs.

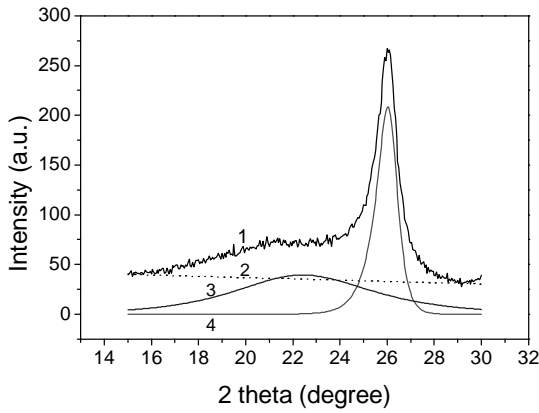


Fig. 8. (1) - experimental XRD spectrum for *c* PPY-CNT; (2) - background correction; (3) - PPY contribution; (4) - line attributed to the reflection on the plane with (002) Miller indices from MWCNTs.

The X-ray line profile (XRLP) for both experimental, $h(2\theta)$, and instrumental, $g(2\theta)$, functions could be approximated by using the so called Generalized Fermi Function (GFF) [10,12]

$$h_{GFF}(2\theta), g_{GFF}(2\theta) = \frac{A}{e^{-a(2\theta-c)} + e^{b(2\theta-c)}} \quad (1)$$

where parameters A and c describe the amplitude and the position of the peak respectively. The parameters a and b control the shape of the XRLP.

The integral widths $\delta_h(a, b)$ and $\delta_g(a, b)$ of the $h(2\theta)$ and $g(2\theta)$ functions respectively are both described by the following type of equation

$$\delta_{h(g)}(a, b) = \frac{\pi}{(a^a b^b)^{1/(a+b)} \cos\left(\frac{\pi a - b}{2 a + b}\right)} \quad (2)$$

Table 2. The best parameters, uncertainties for all distributions.

GFF	$A \pm \delta A$	$a \pm \delta a$	$b \pm \delta b$	$c \pm \delta c$
<i>g</i>	167052 ± 40.2	3.62592 ± 0.16	10.9987 ± 0.04	26.5942 ± 0.0546
<i>h</i> _{MWCNTs}	12197.7 ± 8.65	3.63121 ± 0.244	1.7902 ± 0.08	26.52 ± 0.0265
<i>h</i> _{<i>c</i> PPY-CNT}	3987.73 ± 8.435	1.86319 ± 0.52	3.45473 ± 0.09	26.54 ± 0.02925

Table 3. The integral widths for instrumental, δ_g , experimental, δ_h and true sample, δ_f functions and MWCNTs average crystallite sizes, \bar{D} .

Sample	$\delta_g(a, b)$ [2θ]	$\delta_h(\rho_h, \rho_g)$ [2θ]	$\delta_f(\rho_h, \rho_g)$ [2θ]	\bar{D} [Å]
<i>g</i>	0.53537	-	-	-
MWCNTs	-	1.2687	0.96826	164
<i>c</i> PPY-CNT	-	1.26636	0.99396	159

The description of the microstructure of the systems under investigation is contained into the true sample f function. The true sample function is the solution of the following integral equation

$$h(s) = \int_{-\infty}^{\infty} f(s-t)g(t)dt \quad (3)$$

Here h, f and g functions are expressed in reciprocal space variables s and t . They are related to θ by the usual expression $s = 1/d = 2\sin(\theta)/\lambda$. By solving the integral equation (3) the integral width of the true sample XRLP, δ_f , is obtained as

$$\delta_f(\rho_h, \rho_g) = \frac{\pi}{2\rho_h \cos\left(\frac{\pi\rho_h}{2\rho_g}\right)} \left(\cos\left(\frac{\pi\rho_h}{\rho_g}\right) + 1 \right) \quad (4)$$

where $\rho = (a + b)/2$ for f and g functions respectively.

The average particle size \bar{D} , can be determined by classical Scherrer relation:

$$\bar{D} = \frac{0.9\lambda}{\delta_f \cos(\theta)} \quad (5)$$

where λ is the wavelength of the incident x-ray and θ is the gravity centre of true XRLP.

The parameters of GFF approximation are presented in Table 2. The integral width of experimental and instrumental profiles for each sample and average crystallite sizes are presented in the Table 3. The observed diffraction profile of a standard graphite sample, considered to be free of structural imperfection was used to represent the instrumental g function.

From Table 3 one can see that no significant difference between the average crystallite sizes, \overline{D} for MWCNTs and the nanocomposite *c* PPY-CNT exists. This fact indicates that the crystalline structure of MWCNTs doesn't change significantly by the association with conducting PPY.

4. Conclusions

PPY-CNT nanocomposites have been synthesized by using both previously treated in acids and untreated MWCNTs. By TEM investigations, it was evidenced that PPY-CNT nanocomposites are formed by MWCNTs coated with a thin PPY layer. As a result of the composite formation, significant differences were observed between the IR spectra of PPY and PPY-CNTs especially for the bands ascribed to the pyrrole ring vibrations. This fact could be attributed to the polymer conformational changes at the interface between PPy and the MWCNTs.

A new hybrid nanostructure was obtained by the attachment of Fe₃O₄ nanoparticles on MWCNTs through the PPY polymerization. The easy polymerization of pyrrole monomer on MWCNTs could be an attractive method to attach other different inorganic nanoparticles or functional groups together with a polymer layer.

Acknowledgment

This work was supported by the Romanian Ministry of Education and Research under the research program CERES, project nr. 4-139/2004. We acknowledge the participation in the EU NoE Nanofun-Poly.

References

- [1] M. Hughes, G. Chen, M. Shaffer, D. Fray, A. Windle, *Chem. Mater.* **14**, 1610 (2002).
- [2] Kay Hyeok An, Kwan Ku Jeon, Jeong Ku Heo, Seong Chu Lim, Dong Jae Bae, Young Hee Lee, J. *Electrochem. Soc.* **149**(8), A1058 (2002).
- [3] Mei Gao, Liming Dai, Gordon G. Wallace, *Electroanalysis* **15**, 1089 (2003).
- [4] Yunze Long, Zhaojia Chen, Xuotong Zhang, Jin Zhang, Zhongfan Liu, *J. Phys. D: Appl. Phys.* **37**, 1965 (2004).
- [5] D. Lupu, A. R. Biris, A. Jianu, C. Bunescu, E. Burkel, E. Indrea, G. Mihailescu, S. Pruneanu, L. Olenic, I. Misan, *Carbon* **42**, 503 (2004).
- [6] L. P. Biro, Z. E. Horvath, A. A. Koos, Z. Osvath, Z. Vertesy, Al. Darabont, K. Kertesz, C. Neamtu, Z. S. Sarkozi, L. Tapaszto, *J. Optoelectron. Adv. Mater.* **5**(3), 661 (2003).
- [7] G. Zerbi, M. Gussoni, C. Castiglioni, in *Conjugated Polymers*, J. L. Bredas, R. Silbey (eds.) Kluwer: Dordrecht 1991, pp. 435-507.
- [8] R. G. Davidson, T. G. Turner, *Synthetic Metals* **72**, 121 (1995).
- [9] R. Turcu, W. Graupner, C. Filip, A. Bot, M. Brie, R. Grecu, *Adv. Mater. Opt. Electron.* **9**, 157 (1999).
- [10] N. Aldea, Andreea Gluhoi, P. Marginean, C. Cosma, Xie Yaning, Hu Tiandou, Whongua Wu, Baozhong Dong, *Spectrochim. Acta Part B* **57**, 1453 (2002).
- [11] N. Aldea, C. Tiusan, B. Barz, *J. Optoelectron. Adv. Mater.* **6**(1), 225 (2004).
- [12] N. Aldea, B. Barz, A. C. Gluhoi, P. Margineanu, X. Yaning, H. Tiandou, L. Tao, Z. Wu, *J. Optoelectron. Adv. Mater.* **6**(4), 1287 (2004).

*Corresponding author: rodicat14@yahoo.com